Heliyon 9 (2023) e15818

Contents lists available at ScienceDirect

Heliyon

journal homepage: www.cell.com/heliyon

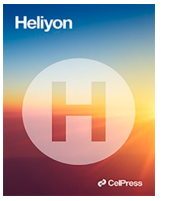

Research article

MiR-21 alleviates renal tubular epithelial cells injury induced by ischemia by targeting TLR4

Xiu-Juan Liu [a,1], Jin-Lei Lv [b,1], Xin Zou [a], Yan-Yan Yu [a], Hong-Xia Zhou [a], Yu Wu [a], Yan-Qiu Geng [c,**], Cai-Hua Lie [d,*]

[a] *Division of Nephrology, The 908 Hospital of Joint Logistics Support Force, Nanchang, Jiangxi, 330000, China*
[b] *Department of Nephrology, The First Affiliated Hospital of Nanchang University, Institute of Molecular Immunology of Kidney Disease of Nanchang University, Nanchang, Jiangxi, 330006, China*
[c] *Division of Nephrology, Third Medical Center of Chinese PLA General Hospital, Beijing, 100039, China*
[d] *Division of Nephrology, General Hospital of Xinjiang Military Region, Urumqi, Xinjiang, 830000, China*

ARTICLE INFO

Keywords:
miR-21
TLR4
AKT
Ischemia
Renal
HIF-1α

ABSTRACT

Renal ischemia is the initial stage of kidney damage, leading to mitochondrial metabolism disorders and cell necrosis. In this study, we aimed to investigate the biological functions and potential mechanisms of miR-21 in protecting renal tubular epithelial cells from oxidative stress and apoptosis following oxygen glucose deprivation (OGD). Following an OGD injury, miR-21 levels increased in HK-2 renal tubular epithelial cells. Overexpression of miR-21 decreased the protein expressions of cleaved caspase-3, BAX, P53, cell apoptosis and increased Bcl-2 expression in HK-2 cells with OGD injury. *In vivo* studies found that miR-21 agomir reduced renal tissue apoptosis, while miR-21 antagomir increased it. In addition, overexpression of miR-21 reduced levels of reactive oxygen species (ROS), malondialdehyde (MDA) and lactate dehydrogenase (LDH) in HK-2 cells with OGD injury. However, miR-21 inhibition exhibited the opposite effect. A dual-luciferase reporter assay demonstrated that miR-21 directly regulates Toll-like receptor 4 (TLR4) by targeting the 3′-UTR of TLR4 mRNA. Overexpression of miR-21 led to decreased TLR4 protein expression, and TLR4 knockdown was shown to greatly increase AKT activity in HK-2 cells by *in vitro* kinase assay. Additionally, TLR4 knockdown promoted AKT phosphorylation and hypoxia-inducible factor-1α (HIF-1α) expression, while TLR4 overexpression inhibited these processes. Furthermore, AKT activation abolished the effect of TLR4 on HIF-1α, while AKT inhibition decreased the expression of TLR4 on HIF-1α in TLR4 knockdown HK-2 cells. Further study revealed that HIF-1α inhibition abolished the protective effect of miR-21 overexpression on ROS, LDH levels and cell apoptosis in HK-2 cells after OGD injury, which is indicated by increased levels of ROS and LDH, as well as increased cell apoptosis after HIF-1α inhibition in miR-21-

Abbreviations: AKT, Protein kinase B; HIF-1α, Hypoxia-inducible factor-1α; I/R, Ischemia-reperfusion; LDH, lactate dehydrogenase; MDA, Malondialdehyde; miRNAs, MicroRNAs; OGD, Oxygen-glucose deprivation; ROS, Reactive oxygen species; siRNA, Small interference RNA; TLR4, Toll-like receptor 4; TUNEL, Terminal deoxynucleotidyl transferase-mediated dUTP nick-end labeling.

* Corresponding author. Division of Nephrology, General Hospital of Xinjiang Military Region, 359 Youhaobei Road, Urumqi, Xinjiang, 830000, China.

** Corresponding author. Division of Nephrology, Third Medical Center of Chinese PLA General Hospital, 69 Yongding Road, Beijing, 100039, China.

E-mail addresses: gengyq1016@163.com (Y.-Q. Geng), caihual30@163.com (C.-H. Lie).

[1] These authors contributed equally to this work (Xiu-Juan Liu and Jin-Lei Lv).

https://doi.org/10.1016/j.heliyon.2023.e15818
Received 21 July 2022; Received in revised form 20 April 2023; Accepted 21 April 2023
Available online 11 May 2023

treated HK-2 cells. In conclusion, miR-21 defends OGD-induced HK-2 cell injury via the TLR4/AKT/HIF-1α axis.

1. Introduction

Renal ischemia is the initial stage of kidney damage, which leads to mitochondrial metabolism disorders and cell necrosis [1]. It often occurs as a consequence of hemorrhagic shock, kidney transplantation, large-vessel surgery, and other factors, resulting in acute kidney injury or even acute renal failure [2,3]. It is well known that severe renal ischemia *in vivo* can impair proximal tubule function and cause afferent arterioles and glomeruli to contract. For instance, renal tubular epithelial cells play a crucial role in clearing apoptotic and necrotic cells, thus preventing further inflammation-related damage. What is more, tubular epithelial cells can dedifferentiate and express innate repair receptors, both of which significantly contribute to the promotion of repair [4,5]. However, prolonged exposure to hypoxia or ischemia can cause tubular epithelial cells to undergo apoptosis and necrosis, impairing kidney function. Therefore, improving the tolerance of renal tubular epithelial cells to oxygen-glucose deprivation (OGD) may be an appropriate management strategy for saving damaged renal tissue and recovering impaired renal function caused by renal ischemia.

MicroRNAs (miRNAs) are small, single-stranded RNAs that are endogenously produced, which bind to the 3′-non-coding region (3′-UTR) of the target gene with their seed sequence, leading to the degradation of the target gene or its inhibition in post-transcriptional translation [6,7]. MiRNAs play a crucial role in the regulation of cell proliferation, apoptosis, and immune-inflammatory reactions [8,9]. MiR-21 was revealed to play a protective role during tissue injury caused by ischemia-reperfusion (I/R). By suppressing P53, miR-21 overexpression reduced neuronal death, and protected against ischemic damage [10]. Upregulation of miR-21 has been observed in renal I/R damage, and miR-21 knockdown has been shown to promote renal cells apoptosis and angiogenesis by negatively regulating thrombospondin-1 [11–13]. However, the significance of miR-21 in alleviating renal ischemia injury remains unclear, and no investigation has examined whether miR-21 improves the OGD tolerance of renal tubular epithelial cells.

Toll-like receptor 4 (TLR4) recognizes pathogen-associated molecular patterns and triggers the body's inflammatory response. TLR4 activation by endogenous extracellular matrix ligands has been studied in various inflammation and tissue injury paradigms. For example, in Alzheimer's disease, inhibition of TLR4 induces M2 microglial polarization and provides neuroprotection via the LRP3 inflammasome [14]. Studies have confirmed that TLR4 plays an important role in the renal I/R process and helps to reduce renal I/R injury by causing a significant number of inflammatory factors to be expressed [15,16]. However, only a few studies have been conducted on the function of TLR4 after renal ischemia. Using bioinformatics analysis, TLR4 was predicted to be a potential target gene of miR-21. Therefore, in our study, we investigated how the interaction between miR-21 and TLR4affects HK-2 cells after OGD damage.

Hypoxia-inducible factor-1α (HIF-1α) is an important transcriptional regulator, and is thought to induce vascular endothelial growth factor [17]. It is extremely significant in the process of I/R injury and is sensitive to ischemia and hypoxia [18]. HIF-1αmediates mitophagy in tubular cells and protects against renal I/R injury via BNIP3 [18]. HIF-1α activation is also necessary during cilastatin preconditioning to prevent renal I/R injury [19]. Moreover, TLR4 may play a role in the activation of protein kinase B (AKT) in murine macrophages [20] and AKT may regulate HIF-1α in hepatocellular cancer [21]. Therefore, we hypothesized that miR-21-mediated AKT/HIF-1α signaling could protect renal tubular epithelial cells from ischemia-induced injury by targeting TLR4.

2. Materials and methods

2.1. Cell culture

HK-2 cells, which are renal tubular epithelial cells, obtained from the American Type Culture Collection (Manassas, VA, USA), was cultured in DMEM/F12 (Gibco, Rockville, MD, USA) and supplemented with 10% (v/v) fetal bovine serum (Gibco), and 100 IU/ml penicillin-streptomycin. The cells were incubated in an atmosphere of 5% CO_2 at 37 °C.

2.2. OGD injury

To mimic ischemia *in vitro*, the cells were subjected to OGD treatment. HK-2 cells were grown in glucose-free DMEM/F12 (Gibco) at 37 °C with 5% CO_2, 1% O_2 and 94% N_2 for 24 h.

2.3. RT-qPCR assay

HK-2 cells and renal tissues were treated with the miRNeasy Mini Kit (Qiagen, Dusseldorf, Germany), and total RNA was extracted. For the analysis of miR-21 expression, RNA was reverse-transcribed into cDNA using the one step Primescript miRNA cDNA Synthesis Kit (Takara, Dalian, China), according to the manufacturer's instructions. For mRNA analysis, total RNA was extracted using TRIzol (Thermo Fisher Scientific, Waltham, MA, USA), and cDNA was synthesized using M-MLV Reverse Transcriptase (Clontech, Palo Alto, CA, USA). RT-qPCR was performed using SYBR Green PCR Master Mix (Applied Biosystems, Carlsbad, CA, USA). The relative expression level was compared with an internal reference gene, i.e., U6 snRNA (for miRNAs) and GAPDH (for mRNA), using the $2^{-\Delta\Delta Ct}$ method.

2.4. Western blot

Cells and renal tissues were lysed with lysis buffer, and equal amounts of protein (25 μg) were separated by 12% sodium dodecyl sulfate polyacrylamide gel electrophoresis. The protein was then transferred onto polyvinylidene fluoride (Millipore, Billerica, MA, USA). The membrane was blocked with 5% non-fat dry milk dissolved in PBS containing 20% Tween-20 for 2.5 h. Next, it was incubated overnight at 4 °C with primary antibodies. The membrane was then incubated with horseradish peroxidase-conjugated secondary antibody (Sigma, St. Louis, MO, USA) for 2 h at room temperature. The proteins were analyzed using a Bio-Rad Chem-iDoc apparatus. The primary antibodies used were as follows: cleaved caspase-3 (Asp175) antibody (#9661, 1:1000); BAX antibody (#2774, 1:1000); Bcl-2 (124) mouse mAb (#15071, 1:100); P53 antibody (#9282, 1:1000); Toll-like receptor 4 (E5D8T) rabbit mAb (#38519, 1:1000); phospho-AKT (Thr308) antibody (#9275,1:1000); AKT antibody (#9272, 1:1000); HIF-1α antibody (#3716, 1:1000); GAPDH (14C10) rabbit mAb (#2118, 1:1000). The primary antibodies were obtained from Cell Signaling Technology (Danvers, MA, USA).

2.5. TUNEL (terminal deoxynucleotidyl transferase-mediated dUTP nick-end labeling) assay

A TUNEL apoptosis detection kit (Beyotime, Nantong, China) was used, following the manufacturer's protocol, to detect apoptosis in HK-2 cells and kidney tissue. Briefly, paraffin embedded renal tissue sections (4 μm) were deparaffinized. After being permeabilized with 20 μg/ml of DNase-free proteinase K at 37 °C for 20 min, the sections were exposed to a TUNEL reaction mixture and incubated at 37 °C for 60 min in the dark. Cells nuclei were stained with DAPI for 5 min. For quantification, the number of TUNEL-positive cells in kidney sections in 10 optical fields in each tissue section was counted, and the number of TUNEL-positive cells per mm^2 was calculated.

HK-2 cells with the indicated treatment were fixed with 4% polyformaldehyde at 4 °C for 25 min. After being permeabilized with 0.2% Triton X-100, the cells were labeled with the TUNEL reaction mixture and incubated at 37 °C for 60 min in the dark. Cells nuclei were stained with DAPI for 5 min. The number of TUNEL-positive HK-2 cells was counted in five different fields by an observer who was unaware of the cell treatment or transfection status.

2.6. Assay of ROS and MDA

To detect the level of reactive oxygen species (ROS), HK-2 cells (at a density of 1×10^5/well) were incubated with carboxy-H_2DFF-DA (Invitrogen, Carlsbad, CA, USA) for 45 min at 37 °C. Thereafter, they were washed twice with serum-free medium and resuspended in OptiMEM I medium (Invitrogen). Fluorescence-positive cells were measured using a flow cytometer (Beckman Coulter, Kraemer Boulevard Brea, CA, USA) with 488 and 530 nm excitation and emission filters, respectively.

Malondialdehyde (MDA) in the culture medium was measured using an MDA assay kit (Beyotime, Nantong, China) in accordance with the manufacturer's instructions. Briefly, HK-2 cells (at a density of 1×10^6/ml) with the indicated treatment were lysed with lysis buffer. After being centrifuged at 12, 000 g for 10 min at 4 °C, the supernatant was collected, and 100 μl of the supernatant was incubated with 200 μl of MDA detection buffer at 100 °C for 15 min. The absorbance was determined using an ELISA reader (Synergy HT, BioTek Instruments, Winooski, VT) at 532 and 500 nm, respectively.

2.7. LDH leakage detection

The lactate dehydrogenase (LDH) leakage in the culture medium supernatant was tested using an LDH cytotoxicity assay kit (Beyotime). Briefly, the transfected cells in a 96-well plate were incubated with 20 μl of LDH release reagent for 1 h. After being centrifuged at 400 g for 5 min, the supernatant was collected and incubated with 60 μl of LDH detection reagent for 30 min at room temperature in the dark. The absorbance was determined using an ELISA reader at 490 nm.

2.8. Recombinant plasmid construction and cell transfection

MiR-21 mimic, miR-21 inhibitor, TLR4 overexpression plasmid (pcDNA3.1-TLR4), TLR4 small interference RNA (siRNA), and HIF-1α siRNA were obtained from GenePharma (Shanghai, China). The pcDNA3.1-TLR4 was generated as follows: the cDNA of full-length TLR4 was amplified (GenBank accession no. U88880). The cDNA was then treated with restriction endonucleases *Eco*RI and *Bam*HI, followed by its insertion into pcDNA.3.1 vector (Invitrogen). Then, the recombinant vector was transformed into competent cells of *E. coli* DH5α strain (Invitrogen), amplified at 37 °C for 12 h, and then extracted for sequencing. After being sequenced, the correct recombinant plasmid was named pcDNA.3.1-TLR4. The sequence for miR-21 mimic is as follows: 5′-UAGCUUAUCAGACUGAUGUUGA-3' (for sense) and 5′-AACAUCAGUCUGAUAAGCUAUU-3' (for antisense). The sequence for the miR-21 inhibitor is 5′-UCAACAUCAGUCUGAUAAGCUA-3'. The sequence of TLR4 siRNA is as follows: 5′-UUUCCAAAUGGAACAAACCCC-3'. The sequence of HIF-1α siRNA is 5′-GCUGGAGACACAAUCAUAUTT-3'. For miR-21 mimic or inhibitor transfection, HK-2 cells were transfected with 50 nM miR-21 mimic (mimic control was used as a negative control), or inhibitor (inhibitor control was used as a negative control) for 24 h using Turbofect (Thermo Fisher Scientific, Waltham, MA, USA). Finally, the cells were incubated at 37 °C in 5% CO_2, 2% O_2, and 93% N_2 for 24 h.

For pcDNA.3.1-TLR4 transfection, HK-2 cells were transfected with 50 nM miR-21 mimic or inhibitor for 24 h using Turbofect (Thermo Fisher Scientific, Waltham, MA, USA). Finally, the cells were incubated at 37 °C in 5% CO_2, 2% O_2, and 93% N_2 for 24 h.

TLR4 siRNA or HIF-1α siRNA transfection was conducted using X-tremeGENE™ siRNA reagent (Roche). Briefly, 3×10^4 cells were

transfected with 2 μl of X-tremeGENE™ siRNA supplemented with 48 μl serum-free medium and 50 pmol TLR4 siRNA or HIF-1α siRNA and cultured at room temperature for 15 min. After 48 h, the transfection efficiency was detected by Western blot. Finally, cells were incubated at 37 °C in 5% CO_2, 2% O_2, and 93% N_2 for 24 h.

With the AKT activation experiments, pcDNA.3.1-TLR4 transfected-HK-2 cells were treated with 10 μM of AKT activator SC79 for 1 h (Abcam, Cambridge, UK, DMSO was used as control) followed by OGD exposure. TLR4 siRNA-transfected HK-2 cells were treated with 20 μM of LY294002 (Abcam) for 1 h to inhibit PI3K and with 10 μM of SH-5 (Abcam) for 1 h to inhibit AKT. After that, the HK-2 cells were exposed to OGD exposure as previously described.

2.9. Dual-luciferase reporter assay

The 3′-UTR and mutated 3′-UTR of TLR4 in the binding sites for miR-21 were amplified and subcloned into the pmirGLO vectors (Invitrogen). The pmirGLO vectors containing wild-type (WT) or mutant-type (MT) 3′-UTR of TLR4 with miR-21 mimic were co-

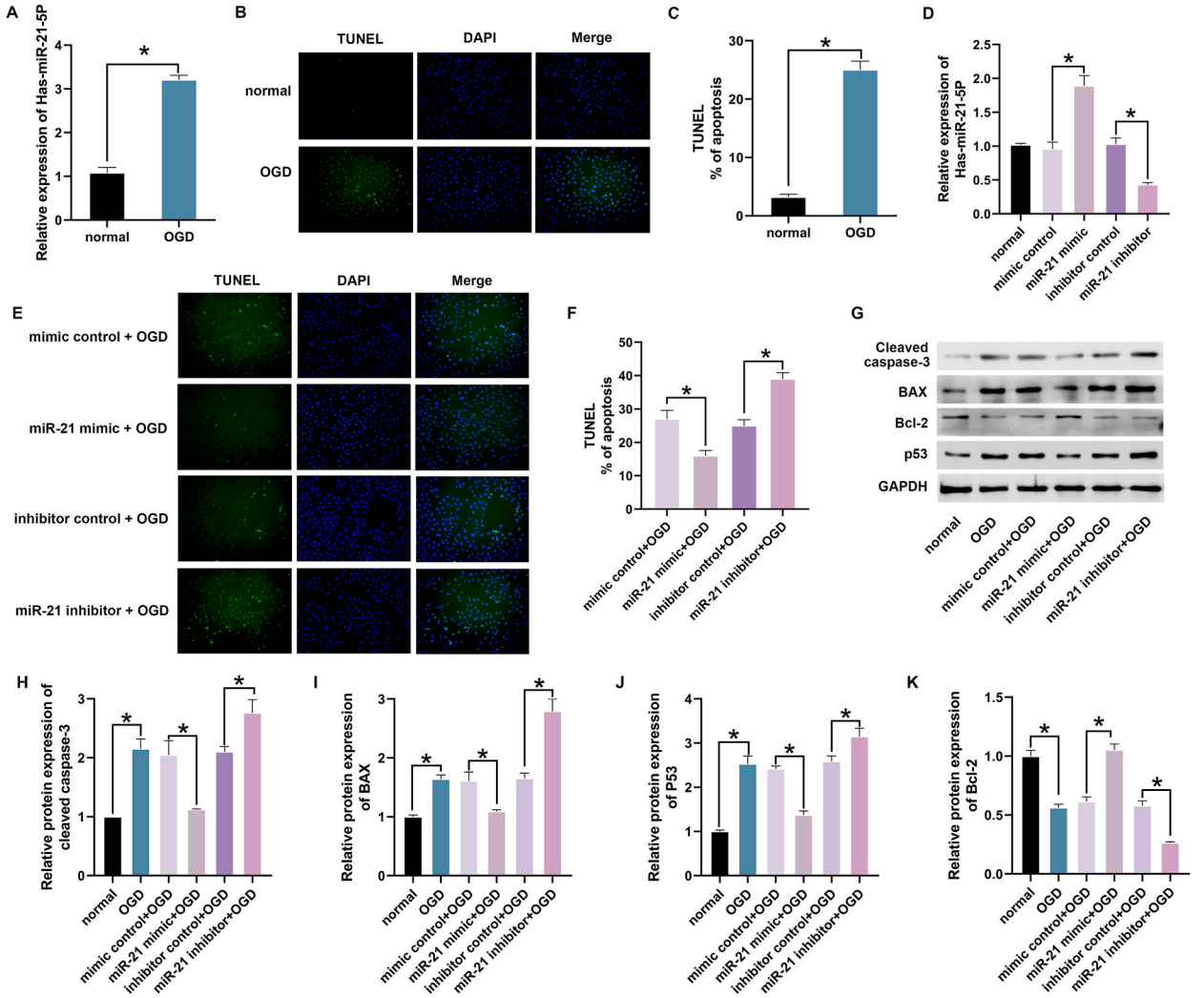

Fig. 1. MiR-21 inhibited cell apoptosis in HK-2 cells induced by OGD. (A) HK-2 cells were subjected to 24 h OGD. The level of miR-21 in HK-2 cells with or without OGD treatment was detected by RT-qPCR. (B) HK-2 cells were subjected to 24 h OGD. Representative images of TUNEL assay. (C) HK-2 cells were subjected to 24 h OGD. Quantity analyses of the percentage of apoptotic cells based on TUNEL assay. (D) HK-2 cells were transfected with miR-21 mimic or miR-21 inhibitor. RT-qPCR was performed to detect the level of miR-21. HK-2 cells were transfected with miR-21 mimic or miR-21 inhibitor, followed by OGD exposure. (E) Representative images of TUNEL assay. (F) Quantity analyses of the percentage of apoptotic cells based on TUNEL assay. (G) The protein expressions of cleaved caspase-3, BAX, P53and Bcl-2 were measured by Western blot. (H–K) Quantity analyses of cleaved caspase-3, BAX, P53, and Bcl-2 in HK-2 cells based on Western blot analyses. Normal, HK-2 cells without OGD injury; OGD, HK-2 cells with OGD injury; mimic control + OGD, mimic control transfected HK-2 cells with OGD treatment; miR-21 mimic + OGD, miR-21 mimic transfected HK-2 cells with OGD treatment; inhibitor control + OGD, inhibitor control transfected HK-2 cells with OGD treatment; miR-21 inhibitor + OGD, miR-21 inhibitor transfected HK-2 cells with OGD treatment. N = 3, $^*P < 0.05$.

transfected into HK-2 cells for 48 h post-transfection. The relative luciferase activity was analyzed using a dual-luciferase system (Promega).

2.10. In vitro kinase assay

The AKT activity in TLR4 siRNA transfected cells was analyzed using an AKT activity assay kit (ab65786; Abcam), according to the manufacturer's instructions. Briefly, HK-2 cells were lysed in ice-cold kinase extraction buffer for 5 min, centrifuged at 13,000 rpm for 10 min at 4 °C, and the protein concentration was determined using the BCA method. Then, 2 μl of AKT-specific antibody and 50 μl of protein A-sepharose were added to 200 μl of cell lysates (300 μg of total cellular protein) and rotated at room temperature for 45 and 60 min, respectively. The mixture was centrifuged, washed with 0.5 ml kinase extraction buffer twice, and washed with 0.5 ml kinase assay buffer once. Thereafter, 2 μl of GSK-3α protein/ATP mixture was added and incubated at 30 °C for 2 h 15 μl of 3 × SDS-PAGE buffer was added to 30 μl of the supernatant. Then, the 45 μl supernatant (containing SDS PAGE buffer) was boiled for 3 min and was extracted. The supernatant (20 μl) was loaded onto a 12% SDS-PAGE gel. Western blotting was performed using the rabbit *anti*-phospho-GSK-3α (Ser 21) specific antibody at 1:1000 dilution. A 37 kDa band corresponding to the phosphorylated GSK-3α should be detected in AKT-activated samples.

2.11. Animals and ischemic treatments

Sprague Dawley (SD) rats were purchased from the Center of Experimental Animals of Nanchang University. Animal experiments were conducted in accordance with a protocol approved by the Institutional Animal Care and Use Committee of Nanchang University. For ischemic treatments, the rats were anesthetized by subcutaneous injection of 2% pentobarbital sodium (60 mg/kg), followed by a ventral incision to expose bilateral renal pedicles. Later, bilateral renal pedicles were exposed for clamping to induce 45 min of ischemia. To avoid reflow following ischemia, the clamps remained in place until the removal of the kidneys. Rats in the sham group underwent the same operation without renal pedicle clamping. For miR-21 treatment, the rats received a tail vein injection with 10 mg/kg miR-21 agomir or antagomir (GenePharma) for 10 days (once a day), following an ischemic treatment.

2.12. Serum creatinine detection

Blood was collected and immediately centrifuged at 3000 g for 10 min at 4 °C to obtain serum for the analysis. The concentrations of serum creatinine were measured with a fully automatic biochemical detector to determine renal function.

2.13. Statistical analysis

All data were expressed as means ± standard error of mean (SEM). Comparisons between groups were made using the one-way ANOVA test followed by Tukey's post-hoc correction in SPSS for Windows, version 21.0. The student's *t*-test was used to compare the mean values of the two groups. A value of $P < 0.05$ was considered statistically significant.

3. Results

3.1. MiR-21 inhibited apoptosis of HK-2 cells induced by OGD

To investigate the effect of OGD on miR-21 in HK-2 cells, the level of miR-21 was measured using RT-qPCR assay. OGD-treated HK-2 cells showed significantly higher levels of miR-21 than the normal group ($P < 0.05$, Fig. 1A). Cell apoptosis was significantly increased in the OGD group compared to the normal group ($P < 0.05$, Fig. 1B and C). To investigate the role of miR-21 in OGD-induced injury, the HK-2 cells were transfected with miR-21 mimic or miR-21 inhibitor to overexpress or downregulate miR-21. The RT-qPCR results revealed that miR-21 mimic transfection increased miR-21 levels and that miR-21 inhibitor transfection decreased miR-21 levels (Fig. 1D). The TUNEL assay was used to evaluate cell apoptosis of HK-2 cells. The data demonstrated that compared to the mimic control + OGD group, miR-21 mimic significantly reduced the apoptosis of HK-2 cells with OGD injury ($P < 0.05$, Fig. 1E and F). Compared to the inhibitor control + OGD group, the miR-21 inhibitor significantly enhanced the apoptosis of HK-2 cells with OGD injury ($P < 0.05$, Fig. 1E and F). Western blot assay demonstrated that compared to the normal group, the protein expressions of cleaved caspase-3 (Fig. 1G and H), BAX (Fig. 1G and I) and P53 (Fig. 1G and J) were significantly increased in the OGD group. The protein expression of Bcl-2 was significantly decreased in the OGD group in HK-2 cells (Fig. 1G and K). Compared to the mimic control + OGD group, overexpression of miR-21 significantly reduced the protein expressions of cleaved caspase-3 (Fig. 1G and H), BAX (Fig. 1G and I), and P53 (Fig. 1G and J), while increased protein expression of Bcl-2 (Fig. 1G and K) in HK-2 cells with OGD injury. However, compared to the inhibitor control + OGD group, miR-21 inhibitor significantly enhanced the protein expressions of cleaved caspase-3 (Fig. 1G and H), BAX (Fig. 1G and I), and P53 (Fig. 1G and J), yet decreased the protein expression of Bcl-2 in HK-2 cells with OGD injury (Fig. 1G and K).

3.2. MiR-21 inhibits oxidative stress and cell cytotoxicity in HK-2 cells induced by OGD

Intracellular ROS and MDA levels were considered as indicators of oxidative stress [22]. Moreover, LDH release is widely used to

detect cytotoxicity [23]. To investigate the effect of miR-21 on oxidative stress and cell cytotoxicity, ROS, MDA, and LDH levels were assessed in HK-2 cells with OGD injury following transfection of miR-21 mimic or inhibitor. The results revealed that compared to the normal group, OGD treatment significantly enhanced the levels of ROS ($P < 0.05$, Fig. 2A), MDA ($P < 0.05$, Fig. 2B), and LDH ($P < 0.05$, Fig. 2C). Compared to the mimic control + OGD group, overexpression of miR-21 significantly reduced ROS ($P < 0.05$, Fig. 2A), MDA ($P < 0.05$, Fig. 2B) and LDH ($P < 0.05$, Fig. 2C) levels in HK-2 cells with OGD treatment. Compared to the inhibitor control + OGD group, the miR-21 inhibitor significantly increased ROS (Fig. 2A), MDA (Fig. 2B), and LDH (Fig. 2C) levels in OGD-treated HK-2 cells. These results indicated that miR-21 inhibits oxidative stress and cell cytotoxicity of HK-2 cells induced by OGD.

3.3. MiR-21 directly targets the 3′-UTR of TLR4

In order to elucidate the underlying molecular mechanism of miR-21 in OGD-induced HK-2 cell injury, we predicted the target genes of miR-21 through bioinformatics analysis. Interestingly, the 3′-UTR of TLR4 had miR-21 binding sites, with the position 666–673 of TLR4 exhibiting a higher absolute value of the context score (Fig. 3A). To investigate whether miR-21 directly targeted TLR4, the position 666–673 of TLR4 3′-UTR was inserted into the luciferase reporter vector with either the wild-type or mutant miR-21 binding site. Then, a dual-luciferase reporter assay was conducted to verify the relationship between miR-21 and TLR4. The dual-luciferase reporter assay indicated that compared to the mimic control group, overexpression of miR-21 significantly restrained luciferase activity in wild-type pGL3-TLR4 3′-UTR (WT) transfected cells, whereas it exhibited no significant effect on luciferase activity in mutated-type pGL3-TLR4 3′-UTR (MT) transfected cells (Fig. 3B). Western blot assay demonstrated that compared to the normal group, the expression of TLR4 was significantly decreased in the OGD group (Fig. 3C). MiR-21 mimic significantly decreased TLR4 protein expression compared to the mimic control + OGD group ($P < 0.05$, Fig. 3C). MiR-21 inhibitor increased TLR4 protein expression compared to the inhibitor control + OGD group ($P < 0.05$, Fig. 3C).

3.4. TLR4 modulates HIF-1α via AKT

OGD treatment led to an increased miR-21 level and a decreased TLR4 level in HK-2 cells. To investigate the role of TLR4 in HK-2 cells with OGD injury, TLR4 was overexpressed via the transfection of pcDNA3.1-TLR4 into HK-2 cells, and TLR4 was silenced via the transfection of TLR4 siRNA into HK-2 cells. Western blot assay showed that compared to the pcDNA3.1-transfected HK-2 cells, the protein expression of TLR4 was significantly increased in pcDNA.3.1-TLR4 transfected HK-2 cells ($P < 0.05$, Fig. 4A). Compared to the si-NC group, the protein expression of TLR4 was significantly decreased in the si-TLR4 group in HK-2 cells ($P < 0.05$, Fig. 4B). GSK-3 is a substrate for the AKT kinase reaction, and the phosphorylation of GSK-3 reflects the activity of AKT. Compared to the si-NC group, TLR4 silencing increased the expression of GSK-3 phosphorylation (Fig. 4C). Compared to the normal group, the protein levels of *p*-AKT and HIF-1α were increased in the OGD group ($P < 0.05$, Fig. 4D, F-G). Compared to the pcDNA3.1 + OGD group, TLR4 overexpression significantly restrained the protein levels of *p*-AKT and HIF-1α in HK-2 cells with OGD injury ($P < 0.05$, Fig. 4D–G). Compared to the si-NC + OGD group, TLR4 silencing significantly increased the protein expressions of *p*-AKT and HIF-1α in HK-2 cells with OGD injury ($P < 0.05$, Fig. 4D–G). Additionally, the AKT activator SC79, which binds to the pleckstrin homology domain of AKT and augments AKT phosphorylation at both the Thr308 and S473 sites [24,25], elevated levels of AKT phosphorylation and HIF-1αin pcDNA3.1-TLR4 transfected HK-2 cells with OGD injury ($P < 0.05$, Fig. 4H and I). Compared to the si-TLR4 + DMSO + OGD group, the specific AKT inhibitor (SH-5) or PI3K inhibitor (LY294002) significantly reduced levels of AKT phosphorylation and HIF-1α in TLR4 siRNA-transfected HK-2 cells with OGD injury ($P < 0.05$, Fig. 4J and K).

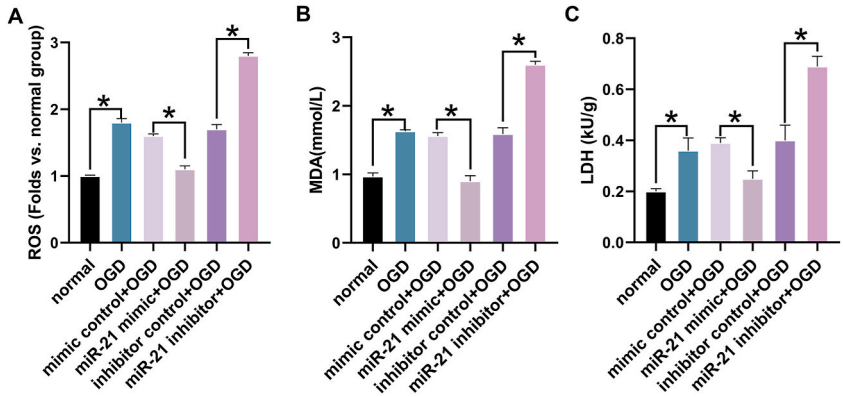

Fig. 2. Effect of miR-21 on oxidative stress and cytotoxicity of HK-2 cells induced by OGD injury. HK-2 cells were transfected with miR-21 mimic or miR-21 inhibitor, followed by OGD exposure. (A) ROS release was measured using a reactive oxygen species assay kit. (B) MDA level in cell supernatant was tested using an MDA assay kit. (C) An LDH assay was performed using an LDH kit. N = 3, *$P < 0.05$.

A

	Predicted consequential pairing of target region (top) and miRNA (bottom)	Site type	Context++ score
Position 666-673 of TLR4 3' UTR	5' . . . UUUUACGUCUUGCCUAUAAGCUA . . .	8 mer	-0.19
hsa-miR-21-5p	3' AGUUGUAGUCAGACUAUUCGAU		
Position 8696-8702 of TLR4 3' UTR	5' . . . AUUUCUGAAAAGGAUUAAGCUAU . . .	7 mer-A1	-0.02
hsa-miR-21-5p	3' AGUUGUAGUCAGACUAUUCGAU		
Position 9049-9055 of TLR4 3' UTR	5' . . . CAAAAGCUUUUAAAUUAAGCUAU . . .	7 mer-A1	-0.02
hsa-miR-21-5p	3' AGUUGUAGUCAGACUAUUCGAU		

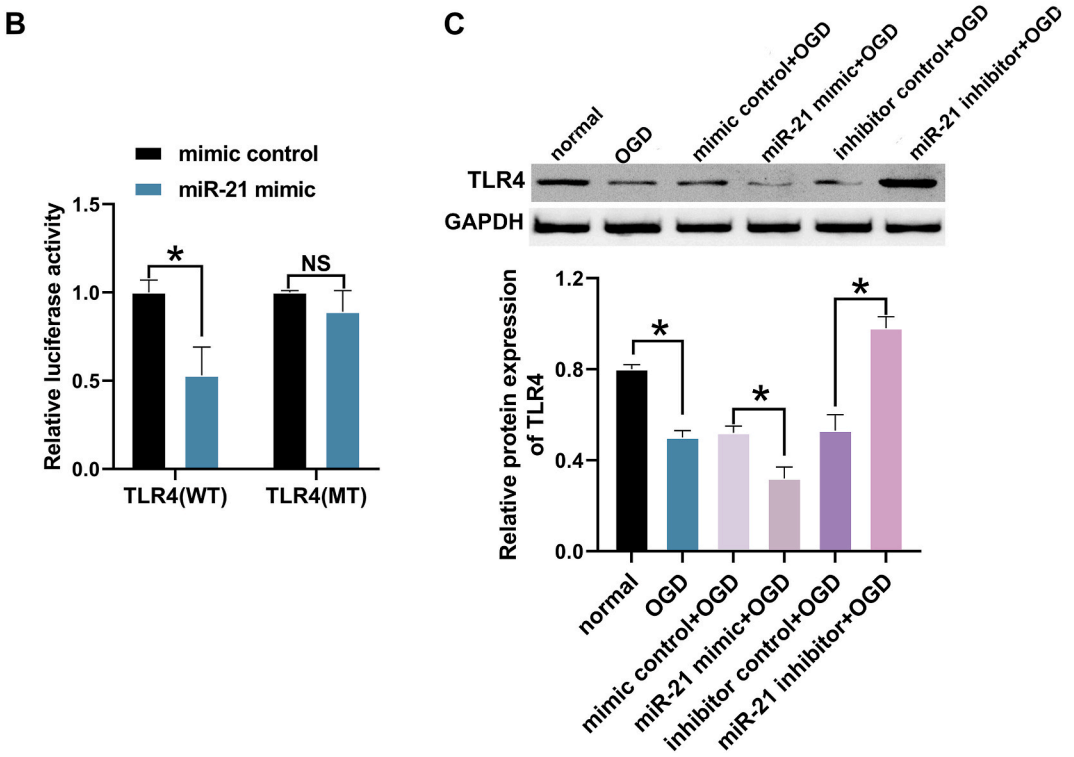

Fig. 3. MiR-21 directly targeted the 3′-UTR of TLR4. (A) The potential miR-21 binding sites on the 3′-UTR of TLR4 predicted by microRNA.org. (B) HK-2 cells were co-transfected with a luciferase reporter vector containing either wild-type (WT) *TLR4* 3′-UTR or mutant (MT) *TLR4* 3′-UTR along with miR-21 mimic. Relative luciferase activity was determined using the dual luciferase reporter assay. (C) HK-2 cells were transfected with miR-21 mimic or inhibitor, followed by OGD exposure. The protein expression of TLR4 was quantified by Western blot. N = 3, $^*P < 0.05$.

3.5. *HIF-1α is involved in the regulation of miR-21 on OGD-induced cell injury*

To investigate the function of HIF-1α in miR-21 mimic-transfected HK-2 cells with OGD injury, HIF-1α siRNA was transfected into HK-2 cells. Western blot assay revealed that compared to miR-21 + OGD + non specific siRNA group, the expression of HIF-1α was inhibited in miR-21 + OGD + HIF-1α siRNA group ($P < 0.05$, Fig. 5A and B). Compared to the miR-21 + OGD + non specific siRNA group, silencing of HIF-1αincreased ROS expression ($P < 0.05$, Fig. 5C) and LDH levels ($P < 0.05$, Fig. 5D) in the miR-21 + OGD + HIF-1α siRNA group. In addition, the TUNEL assay demonstrated that compared to non specific siRNA transfected HK-2 cells, cell apoptosis was significantly increased in HIF-1α siRNA transfected HK-2 cells with OGD injury ($P < 0.05$, Fig. 5E and F).

3.6. *MiR-21 alleviated renal ischemia injury in vivo*

To assess the function of miR-21 *in vivo*, rats were injected with miR-21 agomir or antagomir for 10 days and then subjected to 45 min of bilateral renal ischemia. Compared to the sham group, serum creatinine was significantly increased in the ischemia group, indicating the success of renal ischemia models ($P < 0.05$, Fig. 6A). The expression of miR-21 was significantly increased in the ischemia group compared to the sham group ($P < 0.05$, Fig. 6B). Injection ofmiR-21 agomir significantly increased the level of miR-21, whereas injection of miR-21 antagomir significantly decreased the level of miR-21 ($P < 0.05$, Fig. 6B). Rats treated with miR-21 agomir had reduced serum creatinine levels after renal ischemia compared to the agomir control + ischemia group ($P < 0.05$, Fig. 6A). Rats

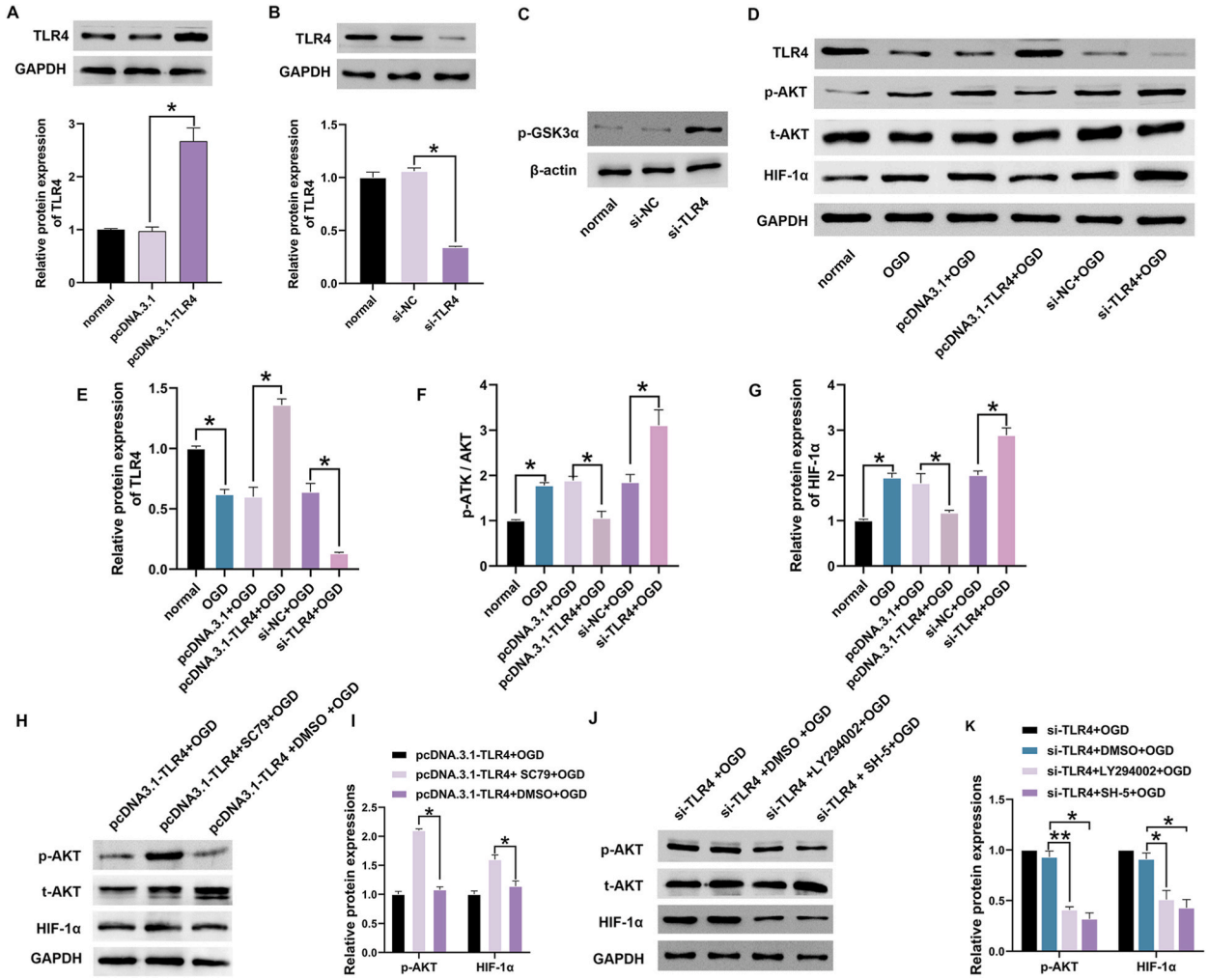

Fig. 4. TLR4 regulated HIF-1α and AKT. (A) HK-2 cells were transfected with pcDNA3.1-TLR4, and the transfection efficiency was analyzed by Western blot. (B) HK-2 cells were transfected with TLR4 small interference RNA (siRNA), and the transfection efficiency was analyzed by Western blot. (C) Western blot assay was used to detect the phosphorylation of GSK-3α, which is a substrate in the AKT kinase reaction. HK-2 cells transfected with pcDNA3.1-TLR4 or TLR4 siRNA were subjected to 24 h of OGD. (D) The protein expressions of TLR4, *p*-AKT, t-AKT, and HIF-1α were tested by Western blot. (E–G) Quantity analyses of TLR4, *p*-AKT/AKT, and HIF-1α in HK-2 cells based on Western blot analyses. (H and I) pcDNA.3.1-TLR4 transfected HK-2 cells were treated with AKT activator SC79 (10 μM) for 1 h, followed by OGD exposure. The protein expressions of *p*-AKT, t-AKT, and HIF-1α were detected by Western blot. (J, K) TLR4 siRNA-transfected HK-2 cells were treated with PI3K inhibitor LY294002 (20 μm) or AKT inhibitor SH-5 (10 μm) for 1 h, followed by OGD exposure. The protein expressions of *p*-AKT, t-AKT, and HIF-1α were detected by Western blot. N = 3, $^*P < 0.05$.

treated with miR-21 antagomir had significantly higher serum creatinine levels after renal ischemia compared to the antagomir control + ischemia group ($P < 0.05$, Fig. 6A). The effect of miR-21 on cell apoptosis was analyzed by TUNEL assay. The data showed that ischemia triggered more apoptosis in comparison to the sham group. MiR-21 agomir significantly reduced apoptosis, while miR-21 antagomir promoted apoptosis ($P < 0.05$, Fig. 6C and D). Additionally, the ratio of *p*-AKT/t-AKT and HIF-1α expression were both clearly higher in the ischemia group compared to the sham group (Fig. 6E). TLR4 expression was significantly lower in the ischemia group compared to the sham group (Fig. 6E). Compared to the agomir control + ischemia group, miR-21 agomir downregulated the expression of TLR4 and increased the ratio of *p*-AKT/t-AKT and HIF-1α expression (Fig. 6E). Compared to the antagomir control + ischemia group, miR-21 antagomir up-regulated the expression of TLR4 and decreased the ratio of *p*-AKT/t-AKT and HIF-1α expression (Fig. 6E).

4. Discussion

The incidence of acute kidney injury caused by renal ischemia occurs particularly frequently [26]. It exacerbates kidney injury by influencing the formation of ROS, cell apoptosis, and the inflammatory activity of several cytokines [27,28]. Renal ischemia is one of

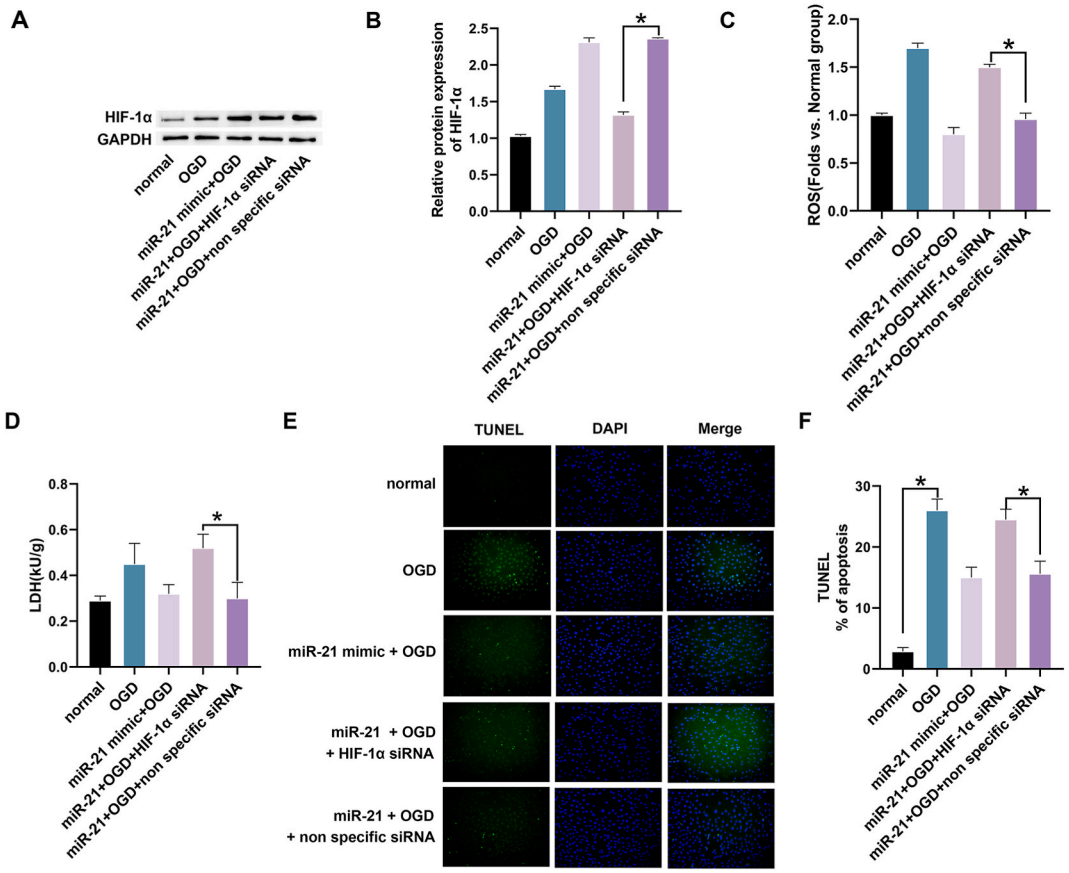

Fig. 5. HIF-1α is involved in the regulation of miR-21 in OGD-induced cell injury. HK-2 cells were co-transfected with miR-21 mimic and HIF-1α siRNA, followed by OGD exposure. (A) The protein expression of HIF-1α was examined by Western blot. (B) Quantity analysis of HIF-1α expression based on Western blot analyses. (C) ROS release was measured using a reactive oxygen species assay kit. (D) An LDH assay was performed using an LDH kit. (E) Representative images of the TUNEL assay. (F) Percentage of apoptotic cells. Normal, HK-2 cells without OGD injury; OGD, HK-2 cells with OGD injury; miR-21 mimic + OGD, miR-21 mimic transfected HK-2 cells with OGD treatment; miR-21 + OGD + HIF-1α siRNA, HIF-1α siRNA was transfected in HK-2 cells with miR-21 overexpression and OGD treatment; miR-21 + OGD + non-specific siRNA, non-specific siRNA was transfected into HK-2 cells with miR-21 overexpression and OGD treatment. N = 3, $^*P < 0.05$ vs. miR-21 + OGD + non-specific siRNA.

the common causes of acute death and disability worldwide [29]. In this study, we discovered that miR-21 was highly expressed in HK-2 cells treated with OGD as well as in the ischemic injured renal tissue of rats. Overexpression of miR-21 inhibited apoptosis and reduced oxidative stress in HK-2 cells via the TLR4/AKT/HIF-1α pathway, while inhibition of miR-21 exhibited the opposite effects.

MiRNA usually acts as a negative regulator of gene expression [6,7]. Various studies found a protective role of miR-21 during I/R-induced tissue injury. For instance, Song et al. [30] discovered that miR-21 alleviated I/R-induced acute kidney injury by inhibiting epithelial cell apoptosis and dendritic cell maturation. By controlling oxidative stress, apoptosis, and other processes in the kidney, miR-21 was implicated in regulating the onset and progression of renal I/R injury [31,32]. Next, Jia et al. [33] demonstrated that inhibition of miR-21 in dendritic cells led to renal I/R damage. Unfortunately, little is known regarding the function of miR-21 following ischemic injury. Furthermore, Li et al. [11] reported that miR-21 may be involved in ischemia pre-treatment protection against I/R-induced kidney injury by targeting the MKK3/IL-6/TNF-α pathway. In this study, we aimed to investigate HK-2 cells injury caused by OGD. As found, miR-21 was elevated after OGD incubation in HK-2 cells. Evidently, after OGD injury, overexpression of miR-21 increased the expression of Bcl-2 in HK-2 cells while suppressing levels of cleaved caspase-3, BAX, and P53 as well as cell apoptosis. Conversely, the miR-21 inhibitor exhibited the opposite results. The accumulation of p53 in the cytosol functioned analogously to the BH3-only subset of proapoptotic Bcl-2 protein to activate BAX and trigger apoptosis [34]. Reduced P53 expression after OGD suggests that p53 is involved in BAX expression induced by OGD. Moreover, miR-21 may protect against OGD-induced HK-2 cells injury by reducing levels of ROS, MDA, and LDH, while miR-21 downregulation may exacerbate OGD-induced HK-2 cells injury. An *in vivo* study demonstrated that overexpression of miR-21 significantly reduced apoptosis, while miR-21 knockdown induced it in renal tissues. Using bioinformatics analysis, we discovered that TLR-4 was a potential target gene of miR-21. Zou et al. [35] found that the miR-21/TLR4/NF-κB signaling pathway might reduce curcumin in lung injury. Additionally, the amelioration of renal I/R injury was closely related to the lowering of TLR-4 expression [36]. We found that miR-21 negatively regulated TLR4 expression in renal tissue with ischemic injury and in HK-2 cells with OGD injury. A dual-luciferase reporter assay further validated the direct interaction

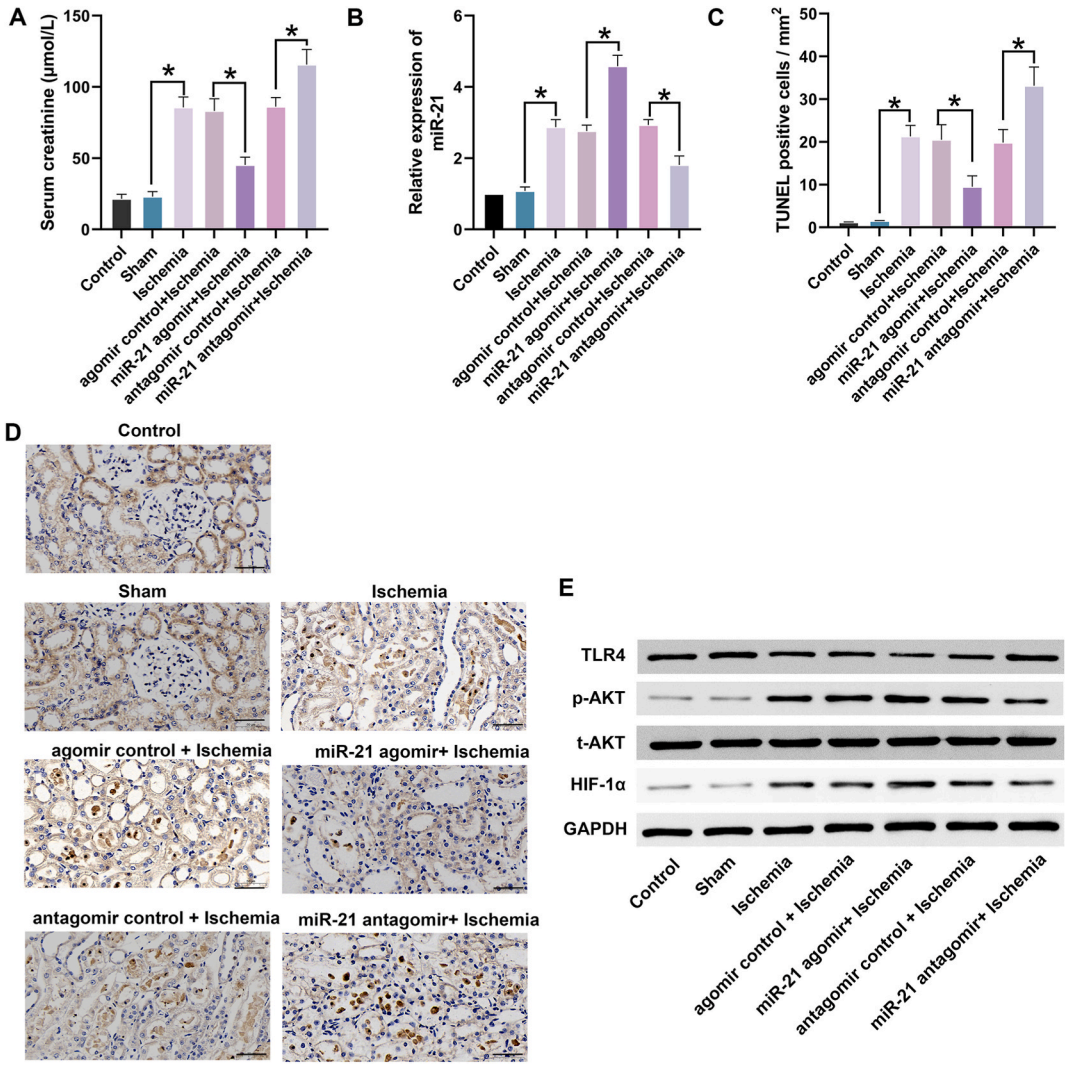

Fig. 6. MiR-21 alleviated renal ischemia injury *in vivo*. Rats were subjected to 45 min of bilateral renal ischemia or sham operation (sham). Kidney tissues were collected for histological and biochemical analysis. (A) Blood samples were collected for the measurement of serum creatinine. (B) Relative expression of miR-21 was detected by RT-qPCR. (C) Percentage of apoptotic cells. (D) Representative images of the TUNEL assay. Scale bar: 50 μm. (E) Quantity analysis of TLR4, *p*-AKT, t-AKT, and HIF-1α expression based on Western blot analyses. $^*P < 0.05$.

between miR-21 and TLR4.

AKT activation could be mediated by TLR4 in murine macrophages [20], and AKT may regulate HIF-1α in hepatocellular carcinoma [21]. HIF-1α mainly regulates the expression of downstream hypoxia-sensitive genes to enable cells to survive under hypoxia [37]. The current study demonstrated that in HK-2 cells with OGD injury, AKT phosphorylation and HIF-1α protein expression were both apparently reduced by TLR4 overexpression, and they were significantly increased by TLR4 knockdown. *In vitro* kinase assay revealed a decrease in AKT activation after TLR4 knockdown. Meanwhile, up-regulation of AKT phosphorylation by SC79 distinctly elevated HIF-1α protein expression. This finding suggested that the up-regulation of AKT phosphorylation could abolish the effect of TLR4 on HIF-1α expression in HK-2 cells with OGD injury. Consequently, TLR4 regulated HIF-1α expression by regulating AKT in HK-2 cells with OGD injury. These findings showed that miR-21 alleviated kidneys from ischemia injury by modulating TLR4/AKT/HIF-1α. Previous research demonstrated that mTOR was an upstream mediator of HIF-1α activation [38], making us speculate that AKT activation induces HIF-1α to be activated via mTOR.

Furthermore, the protective effect of miR-21 on cell apoptosis, ROS, and LDH levels was reversed by HIF-1α inhibition, as shown by the enhanced apoptosis and oxidative stress after HIF-1α siRNA treatment in miR-21 overexpressed HK-2 cells after OGD treatment. The function of HIF-1α following I/R injury was controversial. According to Fu et al. [18], HIF-1α could mediate tubular cell mitophagy and protect against renal I/R injury. Sethi et al. [39] argued that targeting HIF-1α exhibited an inhibitory effect on renal I/R injury. Our results demonstrated a protective role of HIF-1α after a renal ischemic injury. The opposite effect of HIF-1α may be relying on different upstream regulatory genes. To sum up, we first discovered that miR-21 alleviated HK-2 cells OGD injury by targeting the

TLR4 and AKT/HIF-1α axis. HIF-1α could mediate tubular cell mitophagy and protect against renal I/R damage according to Fu et al. [23]. Renal I/R injury were inhibited by HIF-1α targeting. Our findings showed that HIF-1α exhibited a protective effect on renal damage caused by ischemia. The opposing action of HIF-1α may depend on many upstream regulatory genes.

5. Conclusion

This study revealed that miR-21 was elevated in HK-2 cells with OGD. Apoptosis was significantly reduced by miR-21 overexpression both *in vivo* and *in vitr*o. In HK-2 cells with OGD injury, overexpression of miR-21 significantly inhibited oxidative stress, and cell injury. Furthermore, miR-21 could regulate the AKT/HIF-1α axis by modulating TLR4 expression in HK-2 cells with OGD injury, providing further insight into the molecular mechanism of miR-21 in renal injury induced by ischemia.

Credit author statement

Xiu-JuanLiu: Conceptualization, Methodology, Validation, Formal analysis, Investigation, Resources, Writing - Original Draft, Jin-Lei Lv: Conceptualization, Methodology, Validation, Formal analysis, Investigation, Resources, Writing - Original Draft, Xin Zou: Validation, Formal analysis, Investigation- Review & Editing, Yan-Yan Yu: Methodology, Validation, Formal analysis - Review & Editing, Hong-Xia Zhou: Methodology, Validation, Formal analysis - Review & Editing, Yu Wu: Validation, Formal analysis, Investigation- Review & Editing, Yan-Qiu Geng: Software, Formal analysis, Resources, Data Curation, Writing - Review & Editing, Cai-Hua Lie: Software, Formal analysis, Resources, Data Curation, Writing - Review & Editing.

Funding statement

This work was supported by the National Natural Science Foundation of China (No. 81860140), Natural Science Foundation of Jiangxi Province (No. 20181BAB205017), and Science and Technology Project of Jiangxi Provincial Health Commission (No. 202131118).

Data availability statement

The data that support the findings of this study are available from the corresponding author upon reasonable request.

Declaration of competing interest

The authors declare that they have no known competing financial interests or personal relationships that could have appeared to influence the work reported in this paper.

Acknowledgements

None.

References

[1] A.J. Clark, S.M. Parikh, Mitochondrial metabolism in acute kidney injury, Semin. Nephrol. 40 (2) (2020) 101–113.
[2] M. Buleon, M. Cuny, J. Grellier, P.Y. Charles, J. Belliere, A. Casemayou, J.F. Arnal, J.P. Schanstra, I. Tack, A single dose of estrogen during hemorrhagic shock protects against Kidney Injury whereas estrogen restoration in ovariectomized mice is ineffective, Sci. Rep. 10 (1) (2020), 17240.
[3] F. Zhao, X. Wang, T. Liang, D. Bao, Y. Wang, Y. Du, H. Li, J. Du, A. Chen, Z. Fu, Z. Xie, G. Liang, Effect of hyperbaric oxygen on tissue damage and expression of adhesion molecules and C3 in a rat model of renal ischemia-reperfusion injury after kidney transplantation, Ann. Transplant. 25 (2020), e919385.
[4] H. Zhu, W. Jiang, H. Zhao, C. He, X. Tang, S. Xu, C. Xu, R. Feng, J. Li, T. Ma, C. Huang, PSTPIP2 inhibits cisplatin-induced acute kidney injury by suppressing apoptosis of renal tubular epithelial cells, Cell Death Dis. 11 (12) (2020) 1057.
[5] H. Xie, Y. Wang, H. Zhang, Q. Fan, D. Dai, L. Zhuang, R. Tao, Q. Chen, W. Shen, L. Lu, X. Ding, R. Zhang, X. Yan, Tubular epithelial C1orf54 mediates protection and recovery from acute kidney injury, J. Cell Mol. Med. 22 (10) (2018) 4985–4996.
[6] K. Deng, H. Yin, F. Xiong, L. Feng, P. Dong, M. Ren, Genome-wide miRNA expression profiling in potato (Solanum tuberosum L.) reveals TOR-dependent post-transcriptional gene regulatory networks in diverse metabolic pathway, PeerJ 9 (2021), e10704.
[7] R. Kilav-Levin, A. Hassan, M. Nechama, V. Shilo, J. Silver, I.Z. Ben-Dov, T. Naveh-Many, Post-transcriptional mechanisms regulating parathyroid hormone gene expression in secondary hyperparathyroidism, FEBS J. 287 (14) (2020) 2903–2913.
[8] K. Chandan, M. Gupta, M. Sarwat, Role of host and pathogen-derived MicroRNAs in immune regulation during infectious and inflammatory diseases, Front. Immunol. 10 (2019) 3081.
[9] M. Taghavipour, F. Sadoughi, H. Mirzaei, B. Yousefi, B. Moazzami, S. Chaichian, M.A. Mansournia, Z. Asemi, Apoptotic functions of microRNAs in pathogenesis, diagnosis, and treatment of endometriosis, Cell Biosci. 10 (2020) 12.
[10] H. Yan, W. Huang, J. Rao, J. Yuan, miR-21 regulates ischemic neuronal injury via the p53/Bcl-2/Bax signaling pathway, Aging (Albany NY) 13 (18) (2021) 22242–22255.
[11] Z. Li, X. Deng, Z. Kang, Y. Wang, T. Xia, N. Ding, Y. Yin, Elevation of miR-21, through targeting MKK3, may be involved in ischemia pretreatment protection from ischemia-reperfusion induced kidney injury, J. Nephrol. 29 (1) (2016) 27–36.
[12] X. Geng, N. Song, S. Zhao, J. Xu, Y. Liu, Y. Fang, M. Liang, X. Xu, X. Ding, LncRNA GAS5 promotes apoptosis as a competing endogenous RNA for miR-21 via thrombospondin 1 in ischemic AKI, Cell Death Dis. 6 (2020) 19.
[13] X. Xu, N. Song, X. Zhang, X. Jiao, J. Hu, M. Liang, J. Teng, X. Ding, Renal protection mediated by hypoxia inducible factor-1alpha depends on proangiogenesis function of miR-21 by targeting thrombospondin 1, Transplantation 101 (8) (2017) 1811–1819.

[14] W. Cui, C. Sun, Y. Ma, S. Wang, X. Wang, Y. Zhang, Inhibition of TLR4 induces M2 microglial polarization and provides neuroprotection via the NLRP3 inflammasome in Alzheimer's disease, Front. Neurosci. 14 (2020) 444.
[15] J. Bai, J. Zhao, D. Cui, F. Wang, Y. Song, L. Cheng, K. Gao, J. Wang, L. Li, S. Li, Y. Jia, A. Wen, Protective effect of hydroxysafflor yellow A against acute kidney injury via the TLR4/NF-kappaB signaling pathway, Sci. Rep. 8 (1) (2018) 9173.
[16] J.F. Teng, K. Wang, Z.M. Jia, Y.J. Guo, Y.W. Guan, Z.H. Li, X. Ai, Lentivirus-mediated silencing of Src homology 2 domain-containing protein tyrosine phosphatase 2 inhibits release of inflammatory cytokines and apoptosis in renal tubular epithelial cells via inhibition of the TLR4/NF-kB pathway in renal ischemia-reperfusion injury, Kidney Blood Press. Res. 43 (4) (2018) 1084–1103.
[17] Y. Du, Y. Ge, Z. Xu, N. Aa, X. Gu, H. Meng, Z. Lin, D. Zhu, J. Shi, R. Zhuang, X. Wu, X. Wang, Z. Yang, Hypoxia-inducible factor 1 alpha (HIF-1alpha)/Vascular endothelial growth factor (VEGF) pathway participates in angiogenesis of myocardial infarction in muscone-treated mice: preliminary study, Med. Sci. Mon. Int. Med. J. Exp. Clin. Res. 24 (2018) 8870–8877.
[18] Z.J. Fu, Z.Y. Wang, L. Xu, X.H. Chen, X.X. Li, W.T. Liao, H.K. Ma, M.D. Jiang, T.T. Xu, J. Xu, Y. Shen, B. Song, P.J. Gao, W.Q. Han, W. Zhang, HIF-1alpha-BNIP3-mediated mitophagy in tubular cells protects against renal ischemia/reperfusion injury, Redox Biol. 36 (2020), 101671.
[19] Y.A. Hong, S.Y. Jung, K.J. Yang, D.S. Im, K.H. Jeong, C.W. Park, H.S. Hwang, Cilastatin preconditioning attenuates renal ischemia-reperfusion injury via hypoxia inducible factor-1alpha activation, Int. J. Mol. Sci. 21 (10) (2020).
[20] C.P. Bauerfeld, R. Rastogi, G. Pirockinaite, I. Lee, M. Huttemann, B. Monks, M.J. Birnbaum, L. Franchi, G. Nunez, L. Samavati, TLR4-mediated AKT activation is MyD88/TRIF dependent and critical for induction of oxidative phosphorylation and mitochondrial transcription factor A in murine macrophages, J. Immunol. 188 (6) (2012) 2847–2857.
[21] M. Jiao, K.J. Nan, Activation of PI3 kinase/Akt/HIF-1alpha pathway contributes to hypoxia-induced epithelial-mesenchymal transition and chemoresistance in hepatocellular carcinoma, Int. J. Oncol. 40 (2) (2012) 461–468.
[22] G. Coppolino, G. Leonardi, M. Andreucci, D. Bolignano, Oxidative stress and kidney function: a brief update, Curr. Pharmaceut. Des. 24 (40) (2018) 4794–4799.
[23] G. Fotakis, J.A. Timbrell, In vitro cytotoxicity assays: comparison of LDH, neutral red, MTT and protein assay in hepatoma cell lines following exposure to cadmium chloride, Toxicol. Lett. 160 (2) (2006) 171–177.
[24] H. Jo, S. Mondal, D. Tan, E. Nagata, S. Takizawa, A.K. Sharma, Q. Hou, K. Shanmugasundaram, A. Prasad, J.K. Tung, A.O. Tejeda, H. Man, A.C. Rigby, H.R. Luo, Small molecule-induced cytosolic activation of protein kinase Akt rescues ischemia-elicited neuronal death, Proc. Natl. Acad. Sci. U. S. A. 109 (26) (2012) 10581–10586.
[25] X. Liu, G.K. Kiss, S.J. Mellender, H.R. Weiss, O.Z. Chi, Activation of Akt by SC79 decreased cerebral infarct in early cerebral ischemia-reperfusion despite increased BBB disruption, Neurosci. Lett. 681 (2018) 78–82.
[26] J.V. Bonventre, L. Yang, Cellular pathophysiology of ischemic acute kidney injury, J. Clin. Invest. 121 (11) (2011) 4210–4221.
[27] H. Nasrallah, I. Aissa, C. Slim, M.A. Boujbiha, M.A. Zaouali, M. Bejaoui, V. Wilke, H. Ben Jannet, H. Mosbah, H. Ben Abdennebi, Effect of oleuropein on oxidative stress, inflammation and apoptosis induced by ischemia-reperfusion injury in rat kidney, Life Sci. 255 (2020), 117833.
[28] C. Tang, H. Han, M. Yan, S. Zhu, J. Liu, Z. Liu, L. He, J. Tan, Y. Liu, H. Liu, L. Sun, S. Duan, Y. Peng, F. Liu, X.M. Yin, Z. Zhang, Z. Dong, PINK1-PRKN/PARK2 pathway of mitophagy is activated to protect against renal ischemia-reperfusion injury, Autophagy 14 (5) (2018) 880–897.
[29] F. Saeed, M.M. Adil, F. Khursheed, U.A. Daimee, L.A. Branch Jr., G.A. Vidal, A.I. Qureshi, Acute renal failure is associated with higher death and disability in patients with acute ischemic stroke: analysis of nationwide inpatient sample, Stroke 45 (5) (2014) 1478–1480.
[30] N. Song, T. Zhang, X. Xu, Z. Lu, X. Yu, Y. Fang, J. Hu, P. Jia, J. Teng, X. Ding, miR-21 protects against ischemia/reperfusion-induced acute kidney injury by preventing epithelial cell apoptosis and inhibiting dendritic cell maturation, Front. Physiol. 9 (2018) 790.
[31] H. Hu, W. Jiang, X. Xi, C. Zou, Z. Ye, MicroRNA-21 attenuates renal ischemia reperfusion injury via targeting caspase signaling in mice, Am. J. Nephrol. 40 (3) (2014) 215–223.
[32] J.W. Li, L. Wei, Z. Han, Z. Chen, Mesenchymal stromal cells-derived exosomes alleviate ischemia/reperfusion injury in mouse lung by transporting anti-apoptotic miR-21-5p, Eur. J. Pharmacol. 852 (2019) 68–76.
[33] P. Jia, T. Pan, S. Xu, Y. Fang, N. Song, M. Guo, Y. Liang, X. Xu, X. Ding, Depletion of miR-21 in dendritic cells aggravates renal ischemia-reperfusion injury, Faseb. J. 34 (9) (2020) 11729–11740.
[34] J.E. Chipuk, T. Kuwana, L. Bouchier-Hayes, N.M. Droin, D.D. Newmeyer, M. Schuler, D.R. Green, Direct activation of Bax by p53 mediates mitochondrial membrane permeabilization and apoptosis, Science 303 (5660) (2004) 1010–1014.
[35] H.B. Zou, X.F. Sun, The mechanism of curcumin post-treatment relieving lung injuries by regulating miR-21/TLR4/NF-kappaB signalling pathway, J. Int. Med. Res. 48 (11) (2020), 300060520965809.
[36] J. Zhang, Q. Li, Y.R. Zou, S.K. Wu, X.H. Lu, G.S. Li, J. Wang, HMGB1-TLR4-IL-23-IL-17A axis accelerates renal ischemia-reperfusion injury via the recruitment and migration of neutrophils, Int. Immunopharm. 94 (2021), 107433.
[37] Z. Luo, F. Wu, E. Xue, L. Huang, P. Yan, X. Pan, Y. Zhou, Hypoxia preconditioning promotes bone marrow mesenchymal stem cells survival by inducing HIF-1alpha in injured neuronal cells derived exosomes culture system, Cell Death Dis. 10 (2) (2019) 134.
[38] C.C. Hudson, M. Liu, G.G. Chiang, D.M. Otterness, D.C. Loomis, F. Kaper, A.J. Giaccia, R.T. Abraham, Regulation of hypoxia-inducible factor 1alpha expression and function by the mammalian target of rapamycin, Mol. Cell Biol. 22 (20) (2002) 7004–7014.
[39] K. Sethi, K. Rao, D. Bolton, O. Patel, J. Ischia, Targeting HIF-1alpha to prevent renal ischemia-reperfusion injury: does it work? Int J Cell Biol 2018 (2018), 9852791.